Landes Bioscience www.landesbioscience.com

Supplemental Material to:

Stella Oun, Peter Redder, Jean-Philippe Didier, Patrice François, Anna-Rita Corvaglia, Elena Buttazzoni, Caroline Giraud, Myriam Girard, Jacques Schrenzel and Patrick Linder

The CshA DEAD-box RNA helicase is important for quorum sensing control in *Staphylococcus aureus*

2012; 10(1)
http://dx.doi.org/10.4161/rna.22899

www.landesbioscience.com/journals/rnabiology/article/22899/

A

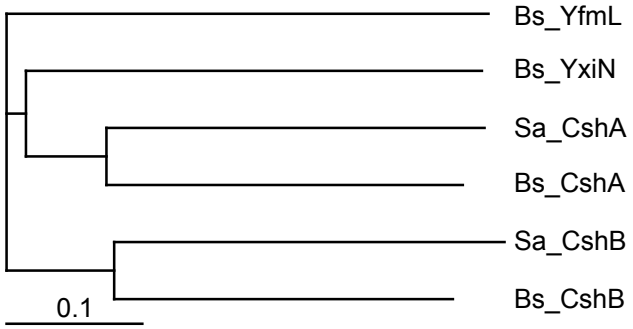
Bs_YfmL
Bs_YxiN
Sa_CshA
Bs_CshA
Sa_CshB
Bs_CshB
0.1

B

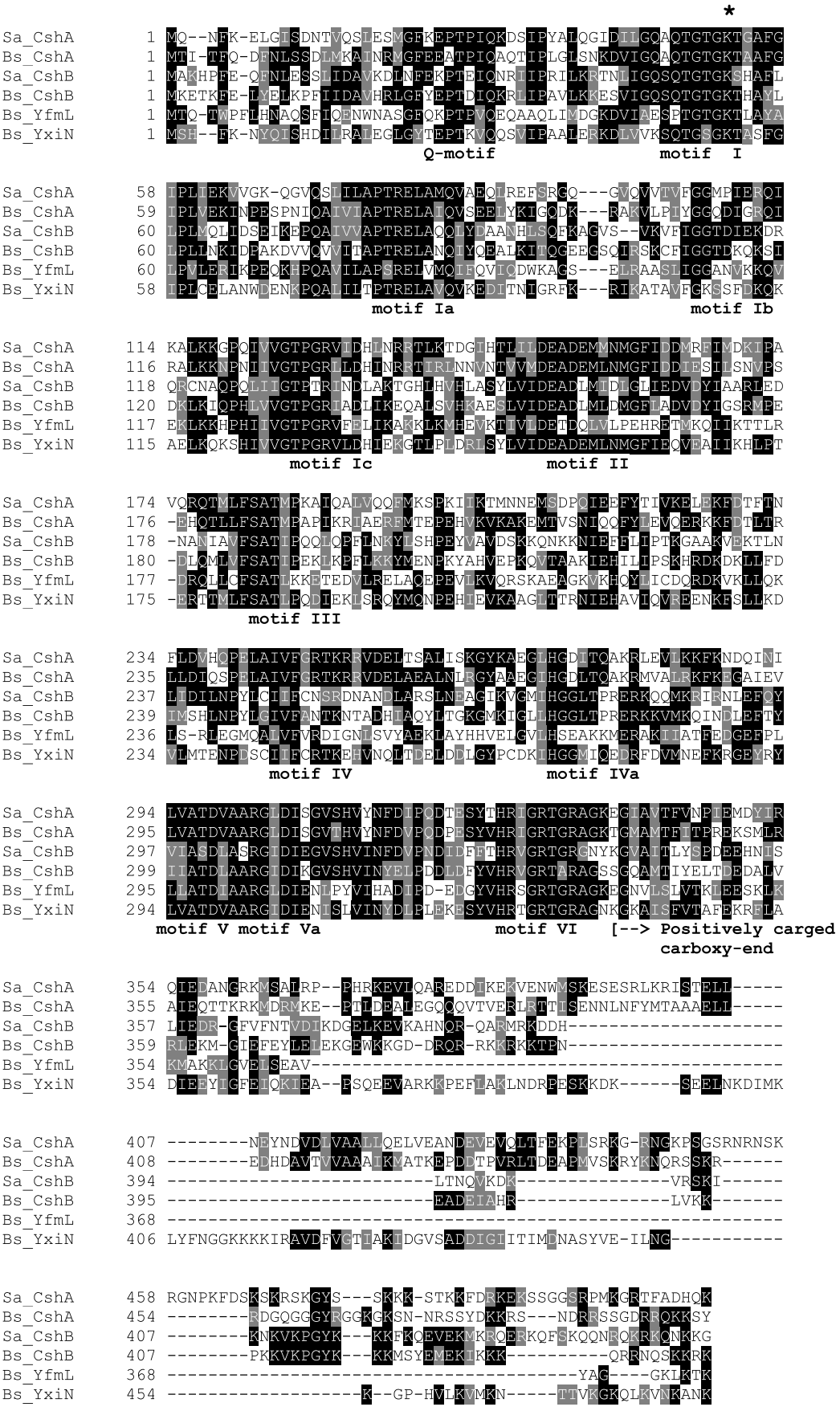
Sa_CshA
Bs_CshA
Sa_CshB
Bs_CshB
Bs_YfmL
Bs_YxiN
Q-motif
motif I
motif Ia
motif Ib
motif Ic
motif II
motif III
motif IV
motif IVa
motif V
motif Va
motif VI
[--> Positively carged carboxy-end

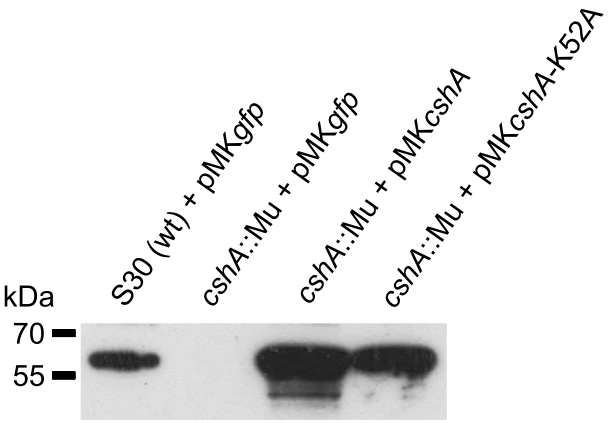
S30 (wt) + pMKgfp
cshA::Mu + pMKgfp
cshA::Mu + pMKcshA
cshA::Mu + pMKcshA-K52A
kDa
70
55

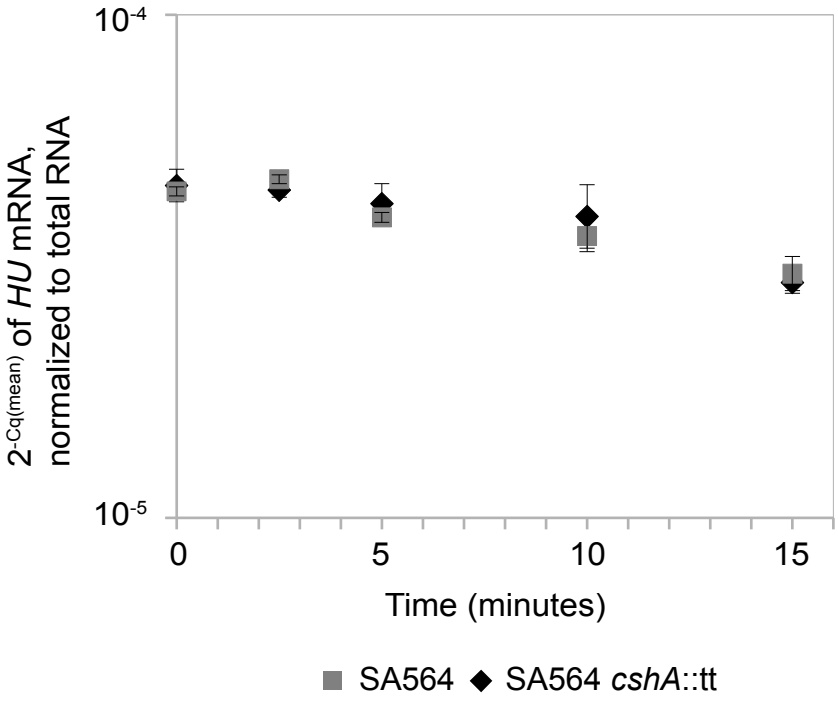
10-4
10-5
2-Cq(mean) of HU mRNA, normalized to total RNA
0
5
10
15
Time (minutes)
SA564
SA564 cshA::tt

S30 *cshA*$^{-}$ *cshA*$^{-}$ *agrA*$^{-}$

A

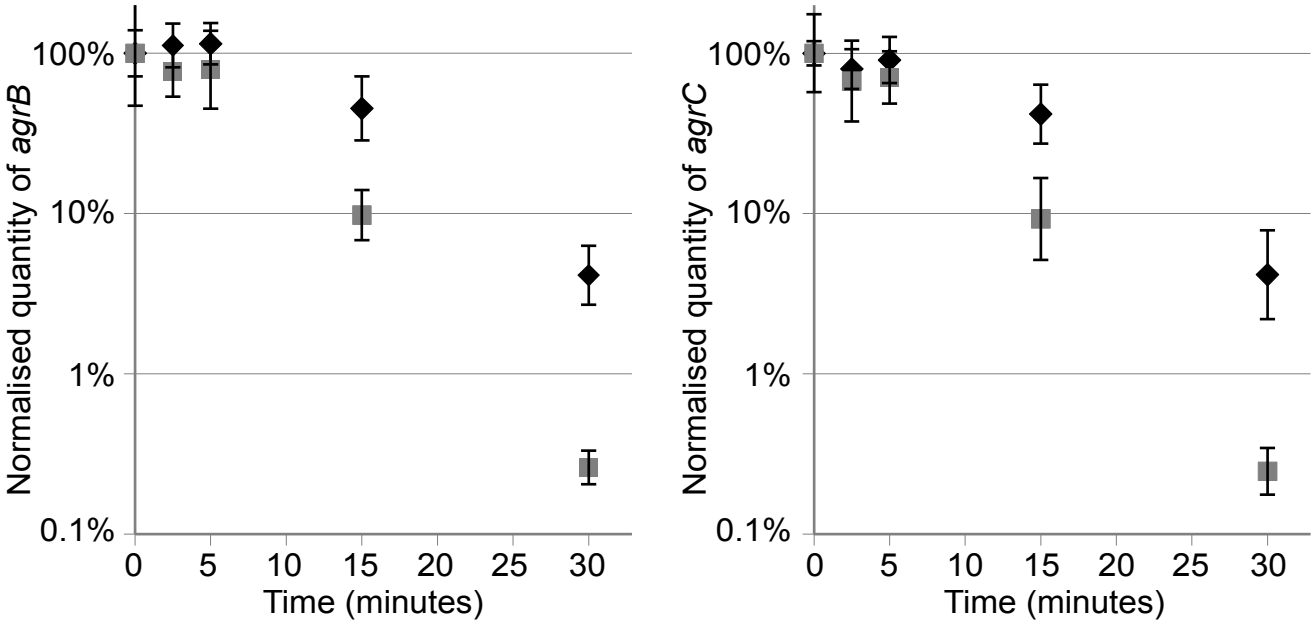
Normalised quantity of agrB
100%
10%
1%
0.1%
0
5
10
15
20
25
30
Time (minutes)
Normalised quantity of agrC
100%
10%
1%
0.1%
0
5
10
15
20
25
30
Time (minutes)

B

S30 ◆ *cshA*⁻


S30 agr region, 4100 bp
qRT-PCR:
B
C
A
agrB
agrD
agrC
agrA

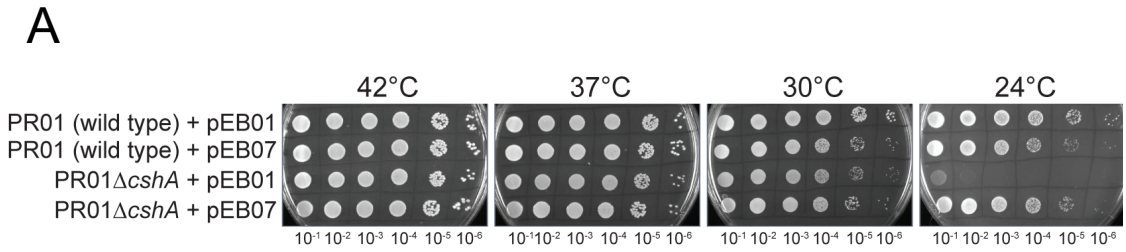
A
42°C
37°C
30°C
24°C
PR01 (wild type) + pEB01
PR01 (wild type) + pEB07
PR01ΔcshA + pEB01
PR01ΔcshA + pEB07
10-1 10-2 10-3 10-4 10-5 10-6

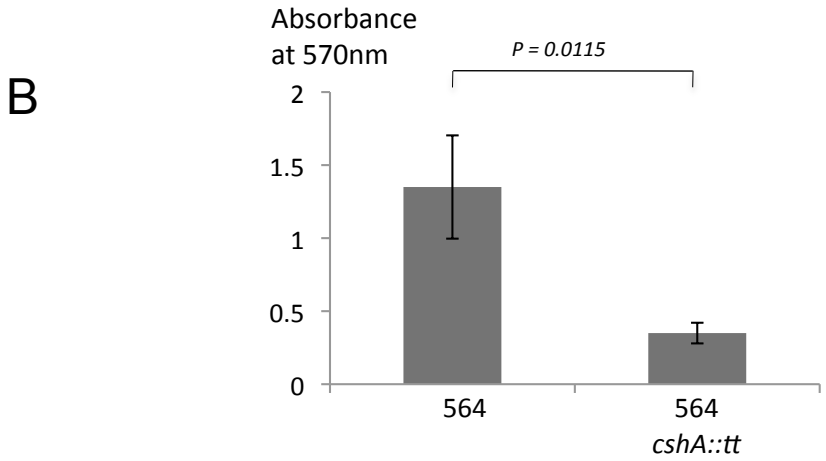
B
Absorbance at 570nm
P = 0.0115
2
1.5
1
0.5
0
564
564 cshA::tt

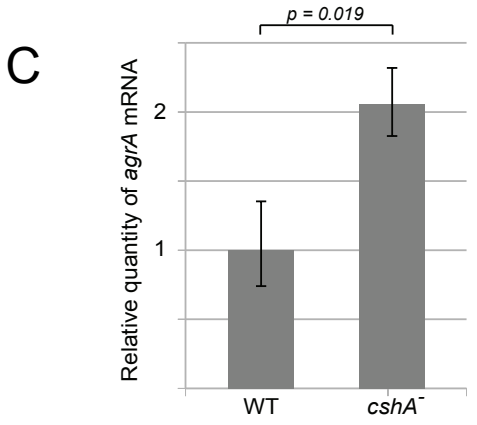
C
p = 0.019
Relative quantity of agrA mRNA
2
1
WT
cshA-

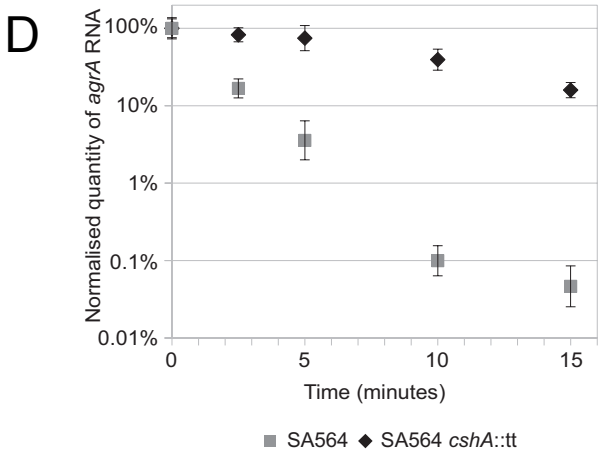
D
Normalised quantity of agrA RNA
100%
10%
1%
0.1%
0.01%
0
5
10
15
Time (minutes)
SA564 SA564 cshA::tt

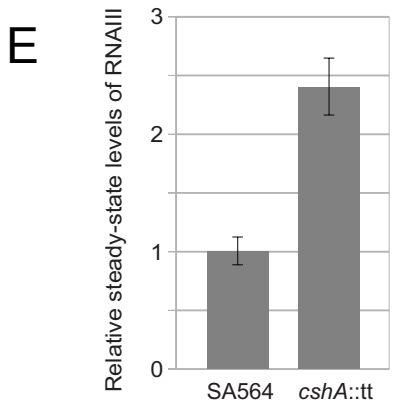
E
Relative steady-state levels of RNAIII
3
2
1
0
SA564
cshA::tt

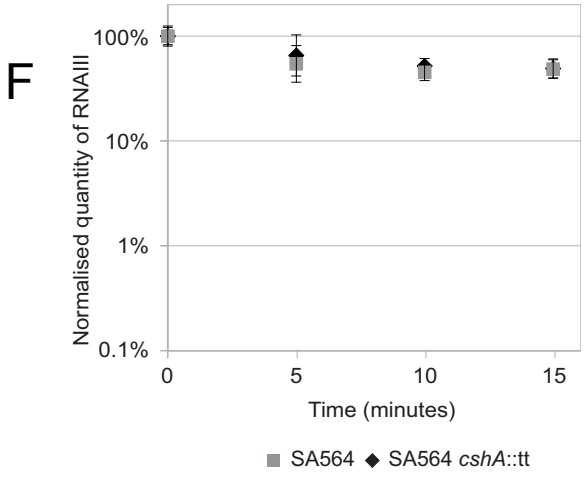
F
Normalised quantity of RNAIII
100%
10%
1%
0.1%
0
5
10
15
Time (minutes)
SA564 SA564 cshA::tt

Supporting Material for:

The CshA DEAD-box RNA helicase is important for quorum sensing control in *Staphylococcus aureus*

Stella Oun*[1], Peter Redder*[1], Jean-Philippe Didier[1], Patrice François[2], Anna Corvaglia[1], Elena Buttazzoni[1], Caroline Giraud[1], Myriam Girard[2], Jacques Schrenzel[2], Patrick Linder[1]

[1] Department of Microbiology and Molecular Medicine, CMU, Medical Faculty, University of Geneva, 1211 Genève 4; Switzerland

[2] Genomic Research Laboratory, Dept of Medical Specialties, Geneva University Hospitals and University of Geneva, 1211 Genève 14; Switzerland

Supporting Figure 1: Alignment of the DEAD-box protein sequences from *Bacillus subtilis* and *Staphylococcus aureus*.

A) Phylogram of the sequences showing the relationship of the different proteins (ClustalW).

B) Alignment of the sequences with the conserved motifs and the C-terminal region indicated. The lysine to alanine change (K52A) in motif I is indicated by an asterisk.

Supporting Figure 2: Western blot analysis of the parental S30 strain, the *cshA*::Mu mutant strain with a plasmid carrying *gfp* as negative control, the mutant strain complemented with the wild type and with the *cshA*-K52A mutant genes. The strains were grown in 1% xylose as for figure 2. The blot was probed using polyclonal rabbit anti-CshA antibodies. Ponceau staining was used to adjust loading of the samples.

Supporting Figure 3: HU mRNA stability is not affected by the *cshA* mutation. RNA was extracted at different time points after rifampicin treatment (as in figure S5D). For qRT-PCR, 2.5 ng of total RNA from each time-point was used to measuring HU mRNA levels, to demonstrate that HU mRNA decay is unaffected by the *cshA* mutation. Grey squares, SA564; Black diamonds, SA564 *cshA*::tt. Error bars represent SD.

Supporting Figure 4: Western blot analysis of alpha hemolysin production. TCA precipitated supernatant of exponentially growing wild type, *cshA* mutant, and *cshA*

agrA double mutant strains were separated on PAGE and analyzed on a Western blot using a commercial anti-alpha-hemolysin antibody.

Supporting Figure 5: A) Decay of *agrB* and *agrC* from S30 measured by qRT-PCR. The mRNAs from S30 (grey squares) and *cshA* mutant (black diamonds) strains were quantified by qRT-PCR after rifampicin treatment as in figure 4. Error bars represent 95% confidence intervals. B) Overview of the *agr* chromosomal region with A, B, and C indicating the positions of the qRT-PCR amplicons.

Supporting figure 6: A) PR01 and the PR01Δ*cshA* mutant with pEB01 (empty vector) and pEB07 (*cshA* containing plasmid) were spotted as in Figure 2 in serial dilutions and grown at the indicated temperature for 2 to 4 days.

B) Biofilm formation is reduced in absence of a functional copy of *cshA* in SA564. Biofilm formation was analyzed as in figure 3A by crystal violet assay. The amount of biofilm was measured after solubilization of the CV in ethanol and absorbance was determined at 570 nm. The difference between the wild type and the mutant was significant ($p = 0.0115$)

C) The *agrA* mRNA level is increased in the SA564 *cshA* mutant strain. Left panel: RNA from these strains was treated as in Figure 4A. Error bars represent SD and an unpaired T-test gave $p = 0.019$.

D) Stability assay of *agrA* mRNA in strain SA564 and the SA564 *cshA* mutant strain, as in Figure 4B and Material and Methods. Error bars represent 95% confidence intervals.

E) Steady state levels of RNAIII are increased in the SA564 *cshA* mutant strain. RNA from wild type and mutant strains was treated as in Figure 4A. Error bars represent SD

F) Stability assay of RNAIII in strain SA564 and the SA564 *cshA* mutant strain was performed as in **D**. The stability is not affected by the *cshA* mutation. Error bars represent 95% confidence intervals.

Supporting Table 1: Oligonucleotides

	Gene	Primer/probe	Sequence	5'label	3'label
qRT-PCR	*HU*	HU_1687F	GGT TTC GGT AAC TTT GAG G		
		HU_1747R	CAG TTT GAG GGT TAC GAC C		
		HU_1708T_FAM	CGT GAA CGT GCT GCA CGT AA	FAM	TAMRA
	agrA	AgrA-34F	CAAAGAGAAAACATGGTTACCATTATTAA		
		AgrA-135R	CTCAAGCACCTCATAAGGATTATCAG		
		AgrA-83T	AAAAGCCTATGGAAATTGCCCTCGCA	FAM	TAMRA
	agrB	AgrB_F	AACAAAATTGACCAGTTTGCCA		
		AgrB_R	CGTACTTGCAAAAATTGAATATGATCTAA		
		AgrB_FAM-MGB	GTATCTTCAAAAGAGAAATAA	FAM	MGB
	agrC	AgrC_type I_70F	CCAGCTATAATTAGTGGTATTAAGTACAGTAAACT		
		AgrC_type I_175R	AGGACGCGCTATCAAACATTTT		
		AgrC_type I_FAM_MGB	ATAGGAATTTCGACATTATC	FAM	MGB
Targetron disruption	*cshA*	97|98a-IBS	AAAAAAGCTTATAATTATCCTTACAAGGCTATCAA GTGCGCCCAGATAGGGTG		
		97|98a-EBS1d	CAGATTGTACAAATGTGGTGATAACAGATAAGTCT ATCAATTTAACTTACCTTTCTTT		
		97|98a-EBS2	TGAACGCAAGTTTCTAATTTCGGTTCCTTGTCGAT AGAGGAAAGTGTCT		
		cshA-verification forward	GCTTACATCTTATCTAATGC		
		cshA-verification reverse	GCTTGGATTGCTTTAGGC		
	cshB	480|481s_IBS	AAAAAAGCTTATAATTATCCTTAGATCTCATGATT GTGCGCCCAGATAGGGTG		
		480|481s_EBS1d	CAGATTGTACAAATGTGGTGATAACAGATAAGTCA TGATTGATAACTTACCTTTCTTTGT		
		480|481s_EBS2	TGAACGCAAGTTTCTAATTTCGATTAGATCTCGAT AGAGGAAAGTGTCT		
	agrA	442|443a-IBS	AAAAAAGCTTATAATTATCCTTACTGAACTACTGC GTGCGCCCAGATAGGGTG		
		442|443a-EBS1d	CAGATTGTACAAATGTGGTGATAACAGATAAGTCT ACTGCCATAACTTACCTTTCTTTGT		
		442|443a-EBS2	TGAACGCAAGTTTCTAATTTCGGTTTTCAGTCGAT AGAGGAAAGTGTCT		
		agrA-verification forward	ATGGTATCGAGAATCTTAAAG		
		agrA-verification reverse	TTAGCGTTTAGCAATCGCG		
Shuttle plasmids	CshA	forward	CGGGTACCAAGGAGGAACAATCTTGCAAAATTTT AAAGAACTAGGGTTTC		
	CshA	backward	AAAACTGCAGTTATTTTTGATGGTCAGCAAATGTG		
	CshA	GAT mutation	GGAATACCGAATGCTCCTGTTGCACCTGTACCGG		
	CshA	GAT mutation	CCGGTACAGGTGCAACAGGAGCATTCGGTATTCC		
Expression plasmids	RNase J1		GGGCATATGAAACAATTACATCCAAATGAAGTAG GTG		
	RNase J1		CGCGGATCCTTATTATTTATTGTTTGATTCTTTTTG TTCGTTTACC		
	RNase J2		GGGCATATGAGTTTAATAAAGAAAAAGAATAAAGA TATTCGC		
	RNase J2		CGCGGATCCTTATTAAATTTCAGAAATTACTGGAA TAATCATAGG		
	CshA		GTA CGA CTA GT C ATA TGC AAA ATT TTA AAG AAC TAG GGA		
	CshA		ACC GTC TCG AGT TTT TGA TGG TCA GCA AAT GTG		